Published on 19 February 2018. Downloaded by Nanjing University of Aeronautics and Astronautics on 2/14/2019 12:44:34 PM.

Biomaterials Science

PAPER

View Article Online
View Journal | View Issue

Check for updates

Cite this: *Biomater. Sci.*, 2018, **6**, 885

Engineering ellipsoidal cap-like hydrogel particles as building blocks or sacrificial templates for three-dimensional cell culture†

Weiwei Zhang,[a] Guoyou Huang, *[b] Kelvin Ng,[b,c] Yuan Ji,[b] Bin Gao,[d] Liqing Huang,[a] Jinxiong Zhou,[f] Tian Jian Lu[b,e,f] and Feng Xu [b]

Received 20th December 2017,
Accepted 19th February 2018

DOI: 10.1039/c7bm01186e

rsc.li/biomaterials-science

Hydrogel particles that can be engineered to compartmentally culture cells in a three-dimensional (3D) and high-throughput manner have attracted increasing interest in the biomedical area. However, the ability to generate hydrogel particles with specially designed structures and their potential biomedical applications need to be further explored. This work introduces a method for fabricating hydrogel particles in an ellipsoidal cap-like shape (*i.e.*, ellipsoidal cap-like hydrogel particles) by employing an open-pore anodic aluminum oxide membrane. Hydrogel particles of different sizes are fabricated. The ability to produce ellipsoidal cap-like magnetic hydrogel particles with controlled distribution of magnetic nanoparticles is demonstrated. Encapsulated cells show high viability, indicating the potential for using these hydrogel particles as structure- and remote-controllable building blocks for tissue engineering application. Moreover, the hydrogel particles are also used as sacrificial templates for fabricating ellipsoidal cap-like concave wells, which are further applied for producing size controllable cell aggregates. The results are beneficial for the development of hydrogel particles and their applications in 3D cell culture.

Introduction

Hydrogels, a polymer network swollen by water without dissolution, have been engineered into various forms including particles, fibers, films and bulk scaffolds for biomedical applications.[1–4] With the development of microengineering technologies, hydrogel particles have attracted increasing interest mainly due to their advantages of small size, spatial compartmentalization, controlled manipulation ability, and easy fabrication.[5,6] Up to now, hydrogel particles have found widespread applications, *e.g.*, as carriers for molecules (*e.g.*, DNA, drug)[7–9] and cell delivery,[10] as building blocks with cells encapsulated for engineering three-dimensional (3D) tissue constructs,[11,12] as sacrificial templates for fabricating porous scaffolds,[13,14] and as smart sensing units for biodetection.[15,16]

Biomedical applications of hydrogel particles depend on their material composition as well as internal and external structures. Commonly used materials for fabricating hydrogel particles include collagen, gelatin, alginate, chitosan, poly (ethylene glycol) (PEG) and poly(vinyl alcohol). Various approaches, including casting molding,[17] photopatterning[18,19] and microfluidics,[20,21] have been developed to engineer hydrogel particles with different structures, such as spherical, cylindrical, cuboid, star- and dumbbell-like structures.[22,23] Moreover, by combining with other material elements (*e.g.*, magnetic nanoparticles (MNPs)), intelligent hydrogel particles having internal controlled structures that can respond to environment stimulation (*e.g.*, magnetic field) have been fabricated.[24,25] Such magnetic-responsive hydrogel particles could be promising building blocks in bottom-up tissue engineering.[26] Nonetheless, despite the remarkable progress in the fabrication and application of hydrogel particles, the capacity for engineering hydrogel particles with specific structures and their potential biomedical applications need to be further explored.

This work reports a nanoporous anodic aluminum oxide (AAO) template-based method to fabricate hydrogel particles in

[a]*Non-equilibrium Condensed Matter and Quantum Engineering Laboratory, The Key Laboratory of Ministry of Education, School of Science, Xi'an Jiaotong University, Xi'an 710049, P.R. China*
[b]*Bioinspired Engineering and Biomechanics Center (BEBC), MOE Key Laboratory of Biomedical Information Engineering, School of Life Science and Technology, Xi'an Jiaotong University, Xi'an 710049, P. R. China. E-mail: wwgyhuang@xjtu.edu.cn*
[c]*Department of Biomedical Engineering, Faculty of Engineering, University of Malaya, Kuala Lumpur 50603, Malaysia*
[d]*Department of Endocrinology and Metabolism, Xijing Hospital, Fourth Military Medical University, Xi'an 710054, P.R. China*
[e]*MOE Key Laboratory for Multifunctional Materials and Structures, Xi'an Jiaotong University, Xi'an 710049, P. R. China*
[f]*State Key Laboratory for Strength and Vibration of Mechanical Structures, School of Aerospace, Xi'an Jiaotong University, Xi'an 710049, P. R. China*
†Electronic supplementary information (ESI) available. See DOI: 10.1039/c7bm01186e

Published on 19 February 2018. Downloaded by Nanjing University of Aeronautics and Astronautics on 2/14/2019 12:44:34 PM.

an ellipsoidal cap-like shape (*i.e.*, ellipsoidal cap-like hydrogel particles). Ellipsoidal cap-like hydrogel particles are of interest since they can not only be used as structure-controlled building blocks for engineering large tissue constructs, but also as sacrificial templates for generating curvature-adjusted concave wells to enhance 3D cell culture. Specifically, AAO membranes with open-pore structures are fabricated and surface-modified to control the ionotropic gelation process of alginate droplets, leading to the generation of ellipsoidal cap-like alginate particles having different sizes. MNPs are further introduced into the hydrogel particles and their distribution is controlled to fabricate ellipsoidal cap-like magnetic hydrogel particles, with the cell encapsulation ability being demonstrated. The hydrogel particles are further used as sacrificial templates for fabricating ellipsoidal cap-like concave wells to promote the formation of size-controlled cell aggregates. The reported approach can be combined with advanced microengineering technologies to greatly benefit 3D cell culture.

Results and discussion

The approach for fabricating ellipsoidal cap-like alginate particles and concave wells is schematically shown in Fig. 1. In this approach, an open-pore AAO membrane with a 3D tiered nanostructure plays a key role in controlling the formation and crosslinking of ellipsoidal cap-like alginate particles. An AAO membrane is a self-organized nanostructure membrane and has found wide applications in many areas, especially in biomedicine.[27,28] The open-pore AAO membrane with a 3D tiered nanostructure used in this work was obtained by using a modified approach.[29,30] Detailed description can be found in the Experimental section.

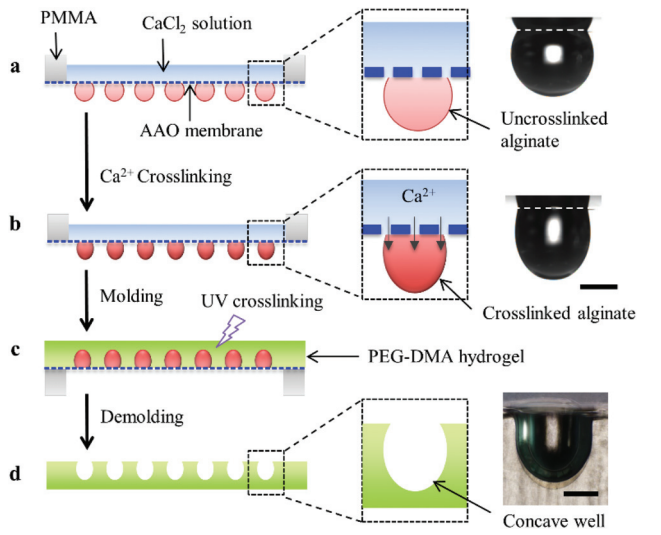

Fig. 1 Schematic illustration of the approach for fabricating ellipsoidal cap-like hydrogel particles and the corresponding concave wells. (a) Generation of uncrosslinked alginate droplets on the AAO membrane back bonded to the PMMA chamber. Right, an uncrosslinked alginate droplet on the AAO membrane with the initial droplet volume of 1 μL. (b) The diffusion of Ca^{2+} through the AAO membrane crosslinks alginate droplets to form hydrogel particles. Right, a crosslinked alginate particle on the AAO membrane with the initial droplet volume of 1 μL. (c) PEG-DMA is applied to cover alginate particles on AAO membrane and UV crosslinks. (d) PEG-DMA hydrogel substrate with ellipsoidal cap-like concave wells is formed by detaching from the AAO membrane and dissolving alginate particles. Right, a concave well formed on the PEG-DMA hydrogel substrate with the initial alginate droplet volume of 1 μL. Scale bars: 500 μm.

Fig. 2a shows the front (top) and back (below) views of the AAO membrane back bonded to a poly(methyl methacrylate) (PMMA) chamber. The PMMA chamber was used to hold calcium chloride ($CaCl_2$) solution for crosslinking alginate droplets (Fig. 1a and b). From scanning electron microscopy (SEM) observation, the front surface of the AAO membrane shows typical hierarchical honeycomb nanostructures, while the back surface shows a single enlarged nanohole pattern (Fig. 2b). The cross-sectional view (Fig. 2c) shows that the AAO membrane has a thickness of ~40 μm, with through nanoholes. These nanoholes endow the AAO membrane with a controlled mass transport property, which is greatly dependent on the molecular weight, pore size and pore surface properties of the AAO membrane.[31] Moreover, the front surface of the open-pore AAO membrane shows a hydrophilic property, with a water contact angle (WCA) of 56.4 ± 1.2° (Fig. 2d, top). After modification with heptadecafluoro-1,1,2,2-tetrahydrodecyl-trichlorosilane (HDFS), the surface becomes hydrophobic, with a WCA of 117.2 ± 2.7° (Fig. 2d, below). High WCAs should be beneficial for the formation of hydrogel droplets and thus the generation of well-shaped hydrogel particles. In addition, the HDFS modification reduces the surface energy of the AAO membrane, enabling easy detachment of alginate particles and the PEG-dimethacrylate (PEG-DMA) hydrogel substrate from the AAO membrane for subsequent studies.

To fabricate hydrogel particles using the AAO membrane, alginate (an anionic polysaccharide typically derived from brown algae) was used due to its biocompatibility, mild, ionotropic and reversible gelation properties. Fig. 3a shows the arrays of alginate hanging droplets on the AAO membrane. When $CaCl_2$ solution was added into the PMMA chamber, Ca^{2+} diffused through the AAO membrane much more quickly than alginate molecules and gradually crosslinked alginate droplets to form hydrogel particles. As shown in Fig. 3b, the morphology of the alginate hanging droplets changed quickly during crosslinking. Several factors, including surface tension, gravity of the droplet and liquid evaporation, may contribute to the morphology evolution of alginate hanging droplets during crosslinking. By controlling the initial droplet volume (varied from 0.5 μL to 1.5 μL in Fig. 3c), the final size of the alginate particles can be easily tuned. As expected and characterized by the contact diameter D, the height H and the radius of curvature R (Fig. 3d), the size of alginate particles increased with increasing initial droplet volume, Fig. 3e and f. Several approaches (*e.g.*, microfluidics and molding) have been developed to generate alginate particles. However, microfluldics cannot generate ellipsoidal cap-like alginate particles and it is cumbersome for the molding method to generate alginate par-

 This journal is © The Royal Society of Chemistry 2018

Published on 19 February 2018. Downloaded by Nanjing University of Aeronautics and Astronautics on 2/14/2019 12:44:34 PM.

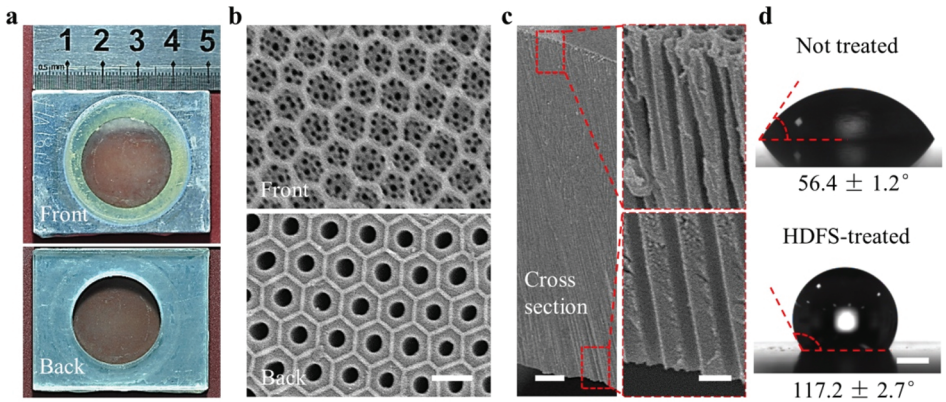

Fig. 2 Characterization of the open-pore AAO membrane. (a) Images of the open-pore AAO membrane back bonded to the PMMA chamber (top, front view; below, back view). (b, c) Microstructure from SEM observation (top in b, front view; below in b, back view; c, cross-sectional view). (d) WCA measurement of the front surface of the AAO membrane (top, before treated with HDFS; below, after treated with HDFS). Scale bars: b, 300 nm; c, 4 μm for left and 200 nm for right; d, 500 μm.

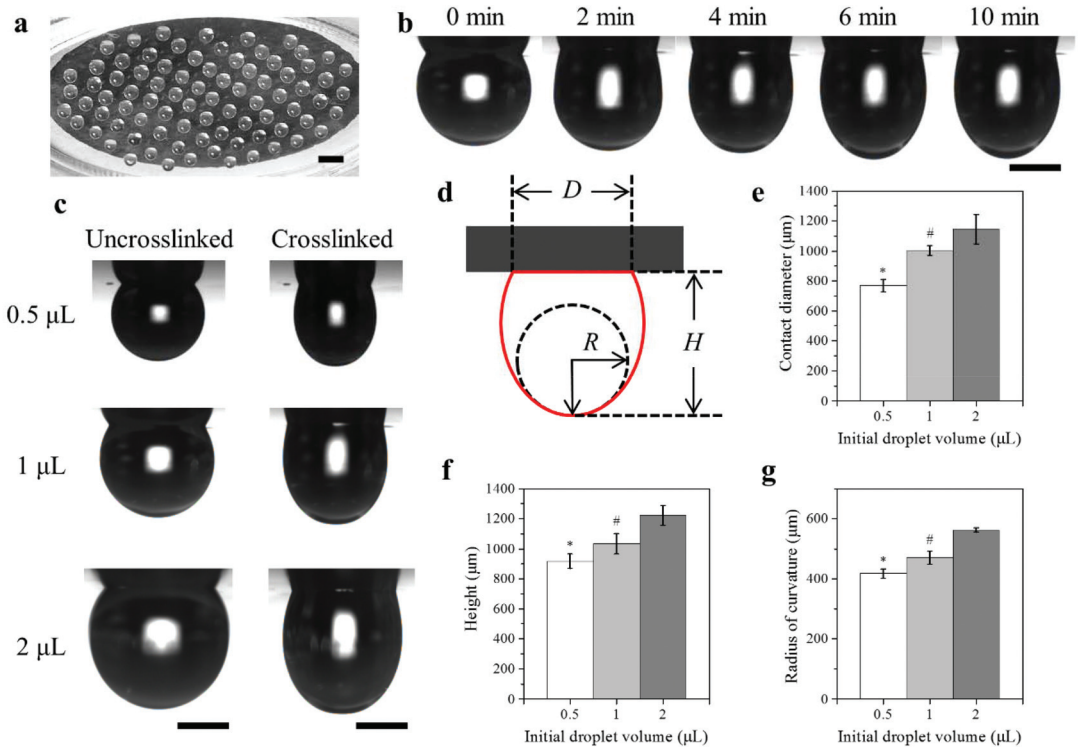

Fig. 3 Formation of alginate particles. (a) Arrays of alginate particles on the AAO membrane. (b) Morphology evolution of an alginate droplet (initial volume = 1 μL) during Ca^{2+} crosslinking. (c) Alginate particles (right) formed from alginate droplets (left) having different initial droplet volumes (*i.e.*, 0.5, 1 and 2 μL). (d) Schematic illustration of the size of crosslinked alginate particles. (e–g) The contact diameter (e), height (f) and radius of curvature (g) of the alginate particles. Scale bars: a, 2 mm; b and c, 500 μm. $^{*}p < 0.05$ relative to 1 μL, $^{\#}p < 0.05$ relative to 2 μL.

ticles of custom-required sizes. In our method, an alternative liquid handling technique such as 3D bioprinting could be used for generating droplets, which would drastically reduce the volume of each droplet and would enable an increased throughput of the method. As the preliminary experimental result, we have generated hydrogel particles with a size of 100–200 μm by using a pressure assisted and value-based 3D bioprinting system we developed previously (ESI Fig. 1†).[32] However, the 3D bioprinting technique is not readily available in common laboratories. Therefore, we used the pipette method that can be widely available to test our idea in the following study.

To demonstrate the potential application of alginate particles as building blocks in tissue engineering, the hydrogel

Published on 19 February 2018. Downloaded by Nanjing University of Aeronautics and Astronautics on 2/14/2019 12:44:34 PM.

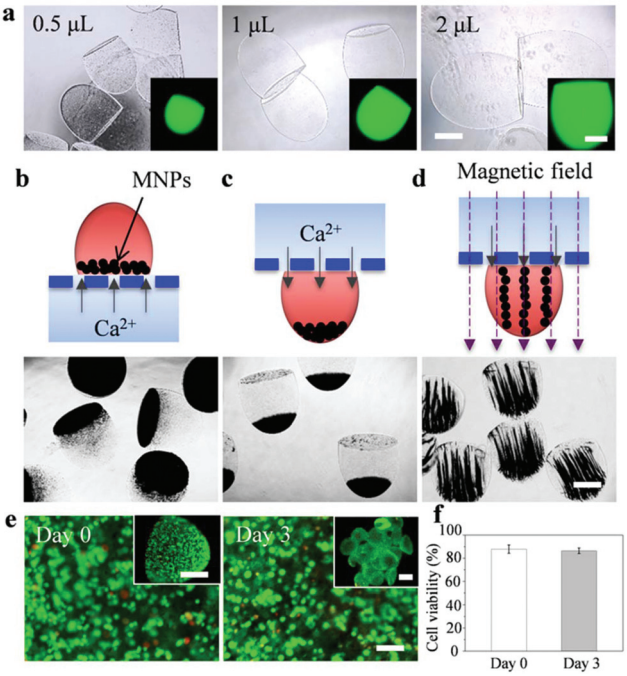

Fig. 4 Potential use of alginate particles as building blocks for bottom-up tissue engineering application. (a) Phase contrast images of freestanding alginate particles of different sizes. Inserts are fluorescent images when FITC loaded. (b–d) Fabrication of magnetic alginate particles with controlled distribution of MNPs. (e) Merged live/dead immunofluorescence images of live (green) and dead (red) cells in magnetic alginate particles. Left, post-encapsulation; right, cultured for 3 days after encapsulation. The magnetic alginate particles on the right (the inset) were assembled into aggregates by applying an external magnetic field. (f) Statistical result of cell viability. Scale bars: a–d, 500 μm; e, 100 μm (inset: left, 500 μm; right, 1 mm).

particles were first detached from the AAO membrane to obtain freestanding forms, Fig. 4a. This not only enables the manipulation of the building block for further study, but also confirms the formation of well-shaped alginate particles. In addition, MNPs were incorporated, with MNPs aggregated either at the bottom (Fig. 4b) or at the top (Fig. 4c) of the ellipsoidal cap-like alginate particles. Moreover, by applying an external uniform magnetic field during alginate crosslinking, the MNPs in alginate particles aligned along the field direction, causing the formation of anisotropic magnetic hydrogel particles, Fig. 4d. Magnetic microgels (*i.e.*, M-gels) have emerged as advanced building blocks in tissue engineering, since they can be manipulated with a magnet in a biocompatible, remote and non-contact manner.[33–35] By controlling the distribution of MNPs in magnetic hydrogel particles, not only the manipulation ability of hydrogel particles can be improved, but the cell–MNP interaction can also be greatly reduced. In the current study, NIH 3T3 mouse embryonic fibroblast cells were encapsulated in magnetic alginate particles during the fabrication process and their viability was evaluated. High cell viabilities (>85%) for NIH-3T3 cells post-encapsulation and cultured for 3 days after encapsulation were observed, demonstrating the biocompatibility of the fabrication process and the hydrogel particles, Fig. 4e, f and ESI Fig. 3.† Further improved cell viability could be achieved by reducing the hydrogel particle size which thus can reduce the crosslinking time and enhance the supply of oxygen and nutrients to the encapsulated cells. Moreover, the cell-laden magnetic alginate particles could be rapidly (in several seconds) assembled to form aggregates by applying a remote external magnetic field (Fig. 4e, the inset at the right), demonstrating their potential application in bottom-up tissue engineering. Although alginate hydrogels cannot inherently support cell adhesion and growth, and are not biodegradable, such difficulties can be overcome by covalently linking cell adhesion ligands (*e.g.*, arginine–glycine–aspartate (RGD)) onto the alginate molecule backbone and partially oxidizing alginate chains, respectively.[12] Alternatively, other biomaterials can also be used and engineered to display physicochemical properties reminiscent of the natural cell microenvironment. For instance, PEG-tyramine macromer,[36,37] hyaluronic acid-tyramine,[38,39] gelatin–hydroxyphenyl propionic acid (GH) and gelatin–hydroxyphenyl propionic acid–tyramine (GHT)[40] can all be enzymatically crosslinked by horseradish peroxidase in the presence of hydrogen peroxide (H_2O_2). These hydrogel systems have shown great promise in tissue engineering and regenerative medicine.[41] We found that H_2O_2 could rapidly diffuse through the AAO membrane in a similar manner to Ca^{2+} (ESI Fig. 2†), indicating that the above-mentioned biomaterials would be compatible with the presented method.

To further demonstrate the application of alginate particles as a sacrificial template for fabricating concave wells, cell-non-adhesive PEG-DMA was used to generate ellipsoidal cap-like concave wells from alginate particles on the AAO membrane. As a widely used synthetic hydrogel for 3D cell culture, PEG-DMA has been recently applied to form concave wells for cell aggregate production.[32] The morphology of cell aggregates strongly depends on the size of concave wells, which, however, is usually controlled by using different templates. Several approaches (*e.g.*, photopatterning and solid template) have been developed to fabricate concave well arrays in hydrogel substrates. However, photopatterning is limited to fabricate concave wells with simple configurations (*e.g.*, flat bottom surfaces) that are not preferential for promoting the generation of uniform-size cell spheroids. Although commercially available solid templates can be used to generate round-bottom well arrays in hydrogel substrates, it is yet cumbersome to generate round-bottom well arrays of varying sizes according to each specific application. Inspired by ice lithography[42] and our previous work on the use of convex gelatin microparticles,[32] we used alginate particles as the sacrificial template for fabricating concave wells since Ca^{2+}-crosslinked alginate can be easily dissolved in the presence of sodium citrate or ethylene diamine tetraacetic acid (EDTA). In our work, ellipsoidal cap-like concave wells of different sizes were easily obtained one time by controlled generation of alginate droplets having different initial volumes on the single AAO membrane, Fig. 5a. The initial droplet volume can be adjusted in accordance with

 This journal is © The Royal Society of Chemistry 2018

Published on 19 February 2018. Downloaded by Nanjing University of Aeronautics and Astronautics on 2/14/2019 12:44:34 PM.

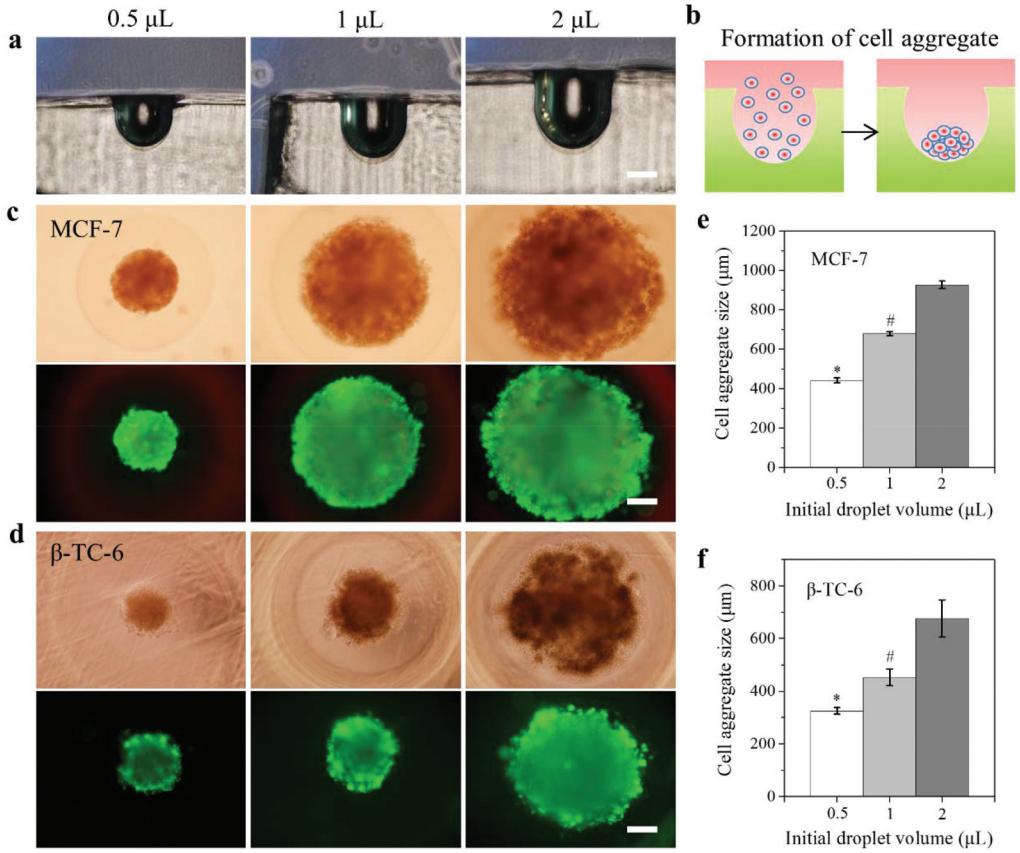

Fig. 5 Fabrication of ellipsoidal cap-like concave wells and the formation of MCF-7 and β-TC-6 cell aggregates. (a) PEG-DMA hydrogel substrates with ellipsoidal cap-like concave wells. (b) Schematic illustration of the formation of cell aggregates in a concave well. (c, d) The formation of (c) MCF-7 and (d) β-TC-6 cell aggregates on day 7 (top, phase contrast images; below, merged live/dead immunofluorescent images after live/dead staining). From left to right, the initial droplet volumes are 0.5, 1 and 2 μL, respectively. (e, f) The diameter of (e) MCF-7 and (f) β-TC-6 cell aggregates. Scale bars: a, 500 μm; c and d, 200 μm. $^{*}p < 0.05$ relative to 1 μL, $^{\#}p < 0.05$ relative to 2 μL.

the special requirement of each experiment. MCF-7 and β-TC-6 cells were employed to separately seed onto the concave wells to generate MCF-7 and β-TC-6 cell aggregates, Fig. 5b. Both MCF-7 (Fig. 5c) and β-TC-6 (Fig. 5d) cells spontaneously self-assembled into closely packed cell aggregates with high cell viability after 7-day culture in the concave wells. By fixing the initial density of cell seeding and varying the size of concave wells (by controlling the initial droplet volume of alginate), cell aggregates with different sizes were obtained. Specifically, the diameter of MCF-7 cell aggregates increased from 442 ± 12 μm to 927 ± 19 μm when the initial droplet volume increased from 0.5 μL to 2 μL (Fig. 5e), while the diameter of β-TC-6 cell aggregates increased from 325 ± 12 μm to 676 ± 71 μm (Fig. 5f). For different concave sizes, the number of cells seeded was different when the initial cell seeding density was fixed. Therefore, it is not surprising that smaller concave wells gave rise to smaller cell aggregates. Moreover, smaller concave wells have a smaller radius of curvature (Fig. 3g), which could also contribute to the formation of smaller compact cell aggregates. The ability to fabricate size-controlled cell aggregates can be further enhanced by employing advanced high-throughput liquid dispersing technologies (*e.g.*, bioprinting) to control the initial droplet volume of alginate. This may greatly promote the development of 3D cell culture models.

Experimental

Substrate preparation and characterization

An open-pore AAO membrane was used as the substrate for controlling the formation of ellipsoidal cap-like hydrogel particles. The AAO membrane was prepared by two-step mild and hard anodization. Briefly, an aluminum (Al) foil substrate (99.99% purity, 200 μm thickness) was cleaned, electropolished, and anodized with mild anodization at 40 V for 5 min and hard anodization at 120 V for 30 min in 0.3 M oxalic acid (AR, Tianjin Hongyan Chemical Reagent Co., Ltd, Tianjin, China) aqueous solutions at −1.5 °C. The AAO membrane was then etched in a mixture solution of 5 wt% phosphoric acid (AR, Tianjin Fuyu Chemical Reagent Co., Ltd, Tianjin, China) and 1.8% chromic acid (AR, Guangdong Guanghua Sci-Tech Co., Ltd, Guangdong, China) at 60 °C for 5 h, followed by a second step of mild anodization at 40 V for 5 min and hard anodization at 120 V for 25 min. After this, the AAO membrane

Published on 19 February 2018. Downloaded by Nanjing University of Aeronautics and Astronautics on 2/14/2019 12:44:34 PM.

was back bonded to the PMMA chamber, which was cut by using a laser etcher (Universal VLS 2.30, Scottsdale, AZ, USA). The residual Al under AAO membranes was removed by filling the PMMA chamber with a saturated cupric chloride (AR, Tianjin Tianli Chemical Reagent Co., Ltd, Tianjin, China) solution. The open-pore AAO membrane was obtained by etching the barrier layer of AAO membranes with a 5 wt% phosphoric acid solution at 35 °C for 120 min. Finally, the front surface of the open-pore AAO membrane was modified with 1/1000 (v/v) HDFS (AR, Aladdin Chemistry CO., Ltd, Shanghai, China) in *n*-hexane (AR, Aladdin Chemistry CO., Ltd, Shanghai, China) to reduce its surface energy by exploiting the high hydrophobic property of HDFS. Before modifying the AAO membrane front surface with HDFS, the PMMA chamber was filled with water to prevent the modification of AAO pores. Without water filling, the pores could also be made hydrophobic, since in this case in the following studies we found that no Ca^{2+} diffused through the AAO membrane to crosslink alginate hanging droplets (data not shown).

The microstructure of the open-pore AAO membrane was characterized with SEM. Briefly, the membrane was broken into small pieces and sputter coated with platinum. The front, back and cross-section of the membrane were examined using a SEM system (SU 8010, Hitachi Ltd, Tokyo, Japan) working at an operating voltage of 5 kV. The images were analyzed with ImageJ 1.49v (NIH, Bethesda, MD, USA). The WCA of the front surface of the AAO membrane was measured with a contact angle goniometer (JGW-360B, Chengde Chenghui Testing Machine Co., Ltd, Chengde, China).

Hydrogel particle fabrication and characterization

To fabricate hydrogel particles, low molecular weight sodium alginate (PROTANAL® LFR 5/60, MW = 35 000 Daltons; kindly supplied by FMC Asia Innovation Center, Shanghai, China) was used. The low viscosity of the sol enables well-controlled generation of small droplets by extrusion or ejection. Sodium alginate is soluble in water and can be ionically crosslinked to form hydrogels rapidly in the presence of divalent (*e.g.*, Ca^{2+}, Zn^{2+} and Ba^{2+}) or trivalent (*e.g.*, Fe^{3+} and Al^{3+}) cations through a high affinity interaction between its G units and the cations.[43] Such crosslinking can be easily removed by using a chelating agent such as sodium citrate and EDTA. Therefore, alginate has been widely used to fabricate hydrogels in the form of fibers and particles.[44,45]

The powder of low molecular weight sodium alginate was completely dissolved in 0.9% (w/v) sodium chloride (NaCl) aqueous solution at a concentration of 15 mg mL^{-1}. The sodium alginate sol was pipetted onto the HDFS-modified front surface of the AAO membrane at different volumes (*i.e.*, 0.5, 1, 2 μL). The AAO membrane was then flipped to form hanging droplets of different sizes. $CaCl_2$ (AR, Aladdin Chemistry CO., Ltd, Shanghai, China) solution (100 mM) was then added into the PMMA chamber to allow the diffusion of Ca^{2+} through the AAO membrane to crosslink alginate hanging droplets. The morphology change of the alginate droplets (particles) was monitored using the optical system of the contact angle goniometer. The alginate particles formed on the AAO membrane were collected in a 12-well plate by water flushing to form freestanding particles, which were viewed under a fluorescent inverted phase contrast microscope (Olympus IX-81, Tokyo, Japan). To obtain fluorescent images, fluorescein isothiocyanate (FITC)-dextran (FD-2000S; Sigma-Aldrich, St Louis, MO, USA) was used during the preparation of alginate particles.

To form magnetic alginate particles, sodium alginate sol was first homogeneously mixed with Fe_3O_4 MNPs (100–300 nm; Aladdin Industrial Inc., Shanghai, China) before pipetting onto the AAO membrane. The final concentrations of sodium alginate and MNPs were 15 mg mL^{-1} and 5 mg mL^{-1}, respectively. The MNPs can spontaneously and rapidly settle to form aggregates at the bottom of the alginate droplets under the action of gravity during hydrogel crosslinking. Moreover, to form anisotropic magnetic alginate particles, an external uniform magnetic field was applied to align MNPs in the alginate droplets during crosslinking.

To explore the use of the presented method with alternative biomaterials such as enzymatically crosslinkable PEG-tyramine macromer, hyaluronic acid-tyramine, GH and GHT, we characterized the diffusion of H_2O_2 (the cross-linking reagent) through the AAO membrane. Deionized water was pipetted onto the HDFS-modified front surface of the AAO membrane at a volume of 5 μL. The AAO membrane was then flipped to form hanging droplets. H_2O_2 aqueous solution (1 M; AR, Tianjin Damao Chemical Reagent Factory, Tianjin, China) was then added into the PMMA chamber to allow the diffusion of H_2O_2 through the AAO membrane. The hanging droplets were collected at selected times and diluted 100 times with acetone for titanium sulfate colorimetry measurement. A series of known concentrations of H_2O_2 were also prepared for titanium sulfate colorimetry measurement to get a standard curve.

3D cell encapsulation and culture

The NIH 3T3 cell line (Cell Bank of the Chinese Academy of Sciences, Shanghai, China), which has been widely used in 3D cell culture,[46,47] was used to demonstrate the cell encapsulation ability of the hydrogel particles. Cells were cultured in high glucose Dulbecco's modified Eagle's medium (DMEM; Gibco-BRL, Grand Island, NY, USA), supplemented with 10% fetal bovine serum (FBS; Gibco-BRL, Grand Island, NY, USA) and a 1% penicillin–streptomycin mixture, and incubated at 37 °C under 5% CO_2. After reaching confluence, the cells were trypsinized, centrifuged and resuspended in 0.9% (w/v) NaCl isotonic saline solution at the concentration of 1.0×10^7 cells per mL. Sodium alginate sol (30 mg mL^{-1}) was filter-sterilized (0.22 μm pore size) and mixed with the above cell suspension at the volume ratio of 1 : 1. The procedure for generating magnetic alginate particles was then applied to obtain cell-laden magnetic alginate particles. Freestanding cell-laden hydrogel particles were cultured with the medium changed every two days.

To characterize the cell viability, cell-laden hydrogel particles post-encapsulation and cultured for 3 days after encapsu-

 This journal is © The Royal Society of Chemistry 2018

Published on 19 February 2018. Downloaded by Nanjing University of Aeronautics and Astronautics on 2/14/2019 12:44:34 PM.

lation were stained for a live/dead assay (Molecular Probes, Eugene, OR, USA) for 15 min at 37 °C according to the manufacturer's instructions. The samples were then imaged using the microscope of Olympus IX-81, with green (under blue excitation) and red (under green excitation) fluorescence indicating live and dead cells, respectively. The cell viability was evaluated based on live/dead immunofluorescence images by calculating the percentage of live (green) cells in magnetic hydrogel particles.

Fabrication of ellipsoidal cap-like concave wells on hydrogels

PEG-DMA (MW = 1000; Polysciences, Inc., Warrington, PA, USA) was applied to form a hydrogel substrate with ellipsoidal cap-like concave wells, considering its non-adhesive property for cells, and easy detachability from the alginate particles and HDFS-modified AAO membrane. After the formation of alginate particles on the AAO membrane, PEG-DMA at the concentration of 15% (w/v) in phosphate buffer solution (PBS) was added to cover the alginate particles and immediately exposed to 365 nm UV light for 60 s with a power of 25 mW cm^{-2} (OmniCure® S2000, Lumen Dynamics, Ontario, Canada). A photoinitiator (PI), 2-hydroxy-2-methylpropiophenone (TCI, Shanghai Development Co., Ltd, Shanghai, China), was used at the concentration of 0.5% (v/v). The crosslinked PEG-DMA with alginate particles was then gently detached from the HDFS-modified AAO membrane and immersed in 75 mM sodium citrate for at least one hour to dissolve alginate, leaving behind ellipsoidal cap-like concave wells on PEG-DMA.

Cell aggregate formation and characterization

MCF-7 and β-TC-6 cells, originating from breast cancer and mouse pancreatic carcinoma, respectively, were both used to demonstrate the formation of cell aggregates on the PEG-DMA hydrogel substrate with ellipsoidal cap-like concave wells. These two kinds of cells are related to some common major diseases and usually work in the form of 3D clusters to maintain their activities. The medium and culture conditions used for culturing MCF-7 were the same as for NIH 3T3, while 15% FBS was used for β-TC-6 instead. The PEG-DMA substrate was washed with PBS three times and UV sterilized before using for cell culture. Sterilized substrates were fixed into 24-well plates and seeded with MCF-7 or β-TC-6 cells at the density of 1.0×10^6 cells per cm^2. The culture medium in the plate of 24 wells was carefully changed every two to three days. Cell aggregates formed in concave wells were imaged with an Olympus IX-81 microscope working in phase contrast mode. In addition, cell aggregates were stained for a live/dead assay (Molecular Probes, Eugene, OR, USA) for 15 min at 37 °C according to the manufacturer's instructions. Fluorescence images were acquired with the Olympus IX-81 microscope, with green (under blue excitation) and red (under green excitation) fluorescence indicating live and dead cells, respectively. Live and dead cell images were evaluated by using ImageJ.

Statistical analysis

All statistical analysis was performed with One-Way ANOVA or a paired sample *t*-test accordingly. Each datum was expressed as mean ± standard deviation (SD) of at least five independent experiments ($n \geq 5$). $p < 0.05$ was accepted as statistically significance.

Conclusions

Hydrogel particles in an ellipsoidal cap-like shape, with or without MNPs incorporated, are fabricated. The potential use of these hydrogel particles as building blocks for tissue engineering application is demonstrated. In addition, ellipsoidal cap-like concave wells are obtained by using alginate particles as the sacrificial template. MCF-7 and β-TC-6 cell aggregates are then generated, which can potentially act as scaffold-free 3D *in vitro* tissue models. Recently, 3D bioprinting technologies have made substantial development. Such advanced technologies can be directly employed to generate droplets, thus enabling the formation of hydrogel particles and concave wells in a well controllable and high-throughput manner. This may greatly broaden the impact and application of the proposed approach in biomedicine.

Conflicts of interest

There are no conflicts to declare.

Acknowledgements

This work was financially supported by the National Natural Science Foundation of China (11602191, 11532009), the Natural Science Basic Research Plan in Shaanxi Province of China (2017JM1026, 2017JM8097), the Industry Key Technologies R&D Project in Shaanxi Province of China (2016GY-209), the Fundamental Research Funds for the Central Universities (8143051) and the Fundamental Research Grant Scheme (FP054-2015A) from the Ministry of Higher Education Malaysia.

References

1 S. R. Caliari and J. A. Burdick, *Nat. Methods*, 2016, **13**, 405–414.
2 D. Seliktar, *Science*, 2012, **336**, 1124–1128.
3 B. V. Slaughter, S. S. Khurshid, O. Z. Fisher, A. Khademhosseini and N. A. Peppas, *Adv. Mater.*, 2009, **21**, 3307–3329.
4 M. Cheng, Y. Wang, L. Yu, H. Su, W. Han, Z. Lin, J. Li, H. Hao, C. Tong, X. Li and F. Shi, *Adv. Funct. Mater.*, 2015, **25**, 6851–6857.

Published on 19 February 2018. Downloaded by Nanjing University of Aeronautics and Astronautics on 2/14/2019 12:44:34 PM.

5 Y. Li, P. Chen, Y. Wang, S. Yan, X. Feng, W. Du, S. A. Koehler, U. Demirci and B.-F. Liu, *Adv. Mater.*, 2016, **28**, 3543–3548.
6 H. Qi, M. Ghodousi, Y. Du, C. Grun, H. Bae, P. Yin and A. Khademhosseini, *Nat. Commun.*, 2013, **4**, 2275.
7 D. Ibraheem, A. Elaissari and H. Fessi, *Int. J. Pharm.*, 2014, **459**, 70–83.
8 L. Hosta-Rigau, O. Shimoni, B. Städler and F. Caruso, *Small*, 2013, **9**, 3573–3583.
9 A. C. Lima, P. Sher and J. F. Mano, *Expert Opin. Drug Delivery*, 2012, **9**, 231–248.
10 Y. Li, W. Liu, F. Liu, Y. Zeng, S. Zuo, S. Feng, C. Qi, B. Wang, X. Yan, A. Khademhosseini, J. Bai and Y. Du, *Proc. Natl. Acad. Sci. U. S. A.*, 2014, **111**, 13511–13516.
11 D. R. Griffin, W. M. Weaver, P. O. Scumpia, D. Di Carlo and T. Segura, *Nat. Mater.*, 2015, **14**, 737–744.
12 S. N. Pawar and K. J. Edgar, *Biomaterials*, 2012, **33**, 3279–3305.
13 Y. Gong, Q. Zhou, C. Gao and J. Shen, *Acta Biomater.*, 2007, **3**, 531–540.
14 Q. Zhou, Y. Gong and C. Gao, *J. Appl. Polym. Sci.*, 2005, **98**, 1373–1379.
15 G. C. Le Goff, R. L. Srinivas, W. A. Hill and P. S. Doyle, *Eur. Polym. J.*, 2015, **72**, 386–412.
16 S. Seiffert, *Angew. Chem., Int. Ed.*, 2013, **52**, 11462–11468.
17 X. Zhang, Z. Meng, J. Ma, Y. Shi, H. Xu, S. Lykkemark and J. Qin, *Small*, 2015, **11**, 3666–3675.
18 K. Cho, H. J. Lee, S. W. Han, J. H. Min, H. Park and W.-G. Koh, *Angew. Chem., Int. Ed.*, 2015, **54**, 11511–11515.
19 U. A. Gurkan, Y. Fan, F. Xu, B. Erkmen, E. S. Urkac, G. Parlakgul, J. Bernstein, W. Xing, E. S. Boyden and U. Demirci, *Adv. Mater.*, 2013, **25**, 1192–1198.
20 I. A. Eydelnant, B. Betty Li and A. R. Wheeler, *Nat. Commun.*, 2014, **5**, 3355.
21 E. Tumarkin and E. Kumacheva, *Chem. Soc. Rev.*, 2009, **38**, 2161–2168.
22 L. Wang, M. Qiu, Q. Yang, Y. Li, G. Huang, M. Lin, T. J. Lu and F. Xu, *ACS Appl. Mater. Interfaces*, 2015, **7**, 11134–11140.
23 A. I. Neto, K. Demir, A. A. Popova, M. B. Oliveira, J. F. Mano and P. A. Levkin, *Adv. Mater.*, 2016, **28**, 7613–7619.
24 Y. Li, G. Huang, B. Gao, M. Li, G. M. Genin, T. J. Lu and F. Xu, *NPG Asia Mater.*, 2016, **8**, e238.
25 A. Doring, W. Birnbaum and D. Kuckling, *Chem. Soc. Rev.*, 2013, **42**, 7391–7420.
26 G. Huang, F. Li, X. Zhao, Y. Ma, Y. Li, M. Lin, G. Jin, T. J. Lu, G. M. Genin and F. Xu, *Chem. Rev.*, 2017, **117**, 12764–12850.
27 W. Lee and S.-J. Park, *Chem. Rev.*, 2014, **114**, 7487–7556.
28 C. J. Ingham, J. ter Maat and W. M. de Vos, *Biotechnol. Adv.*, 2012, **30**, 1089–1099.
29 D. Shan, L. Huang, X. Li, W. Zhang, J. Wang, L. Cheng, X. Feng, Y. Liu, J. Zhu and Y. Zhang, *J. Phys. Chem. C*, 2014, **118**, 23930–23936.
30 J. Wang, L. Huang, L. Zhai, L. Yuan, L. Zhao, W. Zhang, D. Shan, A. Hao, X. Feng and J. Zhu, *Appl. Surf. Sci.*, 2012, **261**, 605–609.
31 S. Cho, S. Lee, S. H. Jeong, Y. Kim, S. C. Kim, W. Hwang and J. Park, *Integr. Biol.*, 2013, **5**, 828–834.
32 K. Ling, G. Huang, J. Liu, X. Zhang, Y. Ma, T. Lu and F. Xu, *Engineering*, 2015, **1**, 269–274.
33 S. Tasoglu, C. H. Yu, H. I. Gungordu, S. Guven, T. Vural and U. Demirci, *Nat. Commun.*, 2014, **5**, 4702.
34 F. Xu, C. A. M. Wu, V. Rengarajan, T. D. Finley, H. O. Keles, Y. R. Sung, B. Q. Li, U. A. Gurkan and U. Demirci, *Adv. Mater.*, 2011, **23**, 4254–4260.
35 R. Turcu, V. Socoliuc, I. Craciunescu, A. Petran, A. Paulus, M. Franzreb, E. Vasile and L. Vekas, *Soft Matter*, 2015, **11**, 1008–1018.
36 D. J. Menzies, A. Cameron, T. Munro, E. Wolvetang, L. Grøndahl and J. J. Cooper-White, *Biomacromolecules*, 2013, **14**, 413–423.
37 K. Ren, B. Li, Q. Xu, C. Xiao, C. He, G. Li and X. Chen, *Polym. Chem.*, 2017, **8**, 7017–7024.
38 K. Xu, F. Lee, S. J. Gao, J. E. Chung, H. Yano and M. Kurisawa, *J. Controlled Release*, 2013, **166**, 203–210.
39 W. S. Toh, T. C. Lim, M. Kurisawa and M. Spector, *Biomaterials*, 2012, **33**, 3835–3845.
40 Y. Lee, J. W. Bae, D. H. Oh, K. M. Park, Y. W. Chun, H.-J. Sung and K. D. Park, *J. Mater. Chem. B*, 2013, **1**, 2407–2414.
41 F. Lee, K. H. Bae and M. Kurisawa, *Biomed. Mater.*, 2015, **11**, 014101.
42 J. Y. Park, C. M. Hwang and S.-H. Lee, *Biomed. Microdevices*, 2009, **11**, 129–133.
43 C. H. Yang, M. X. Wang, H. Haider, J. H. Yang, J.-Y. Sun, Y. M. Chen, J. Zhou and Z. Suo, *ACS Appl. Mater. Interfaces*, 2013, **5**, 10418–10422.
44 K. Y. Lee and D. J. Mooney, *Prog. Polym. Sci.*, 2012, **37**, 106–126.
45 H. Onoe, T. Okitsu, A. Itou, M. Kato-Negishi, R. Gojo, D. Kiriya, K. Sato, S. Miura, S. Iwanaga, K. Kuribayashi-Shigetomi, Y. T. Matsunaga, Y. Shimoyama and S. Takeuchi, *Nat. Mater.*, 2013, **12**, 584–590.
46 Y. Li, G. Huang, M. Li, L. Wang, E. L. Elson, T. J. Lu, G. M. Genin and F. Xu, *Sci. Rep.*, 2016, **6**, 19550.
47 G. Huang, X. Zhang, Z. Xiao, Q. Zhang, J. Zhou, F. Xu and T. J. Lu, *Soft Matter*, 2012, **8**, 10687–10694.

 This journal is © The Royal Society of Chemistry 2018